Vibration-based structural health monitoring of stay cables by microwave remote sensing

Carmelo Gentile*[1] and Alessandro Cabboi[2a]

[1] *Politecnico di Milano, Department of Architecture, Built environment and Construction engineering (ABC), P.za Leonardo da Vinci 32, 20133 Milan, Italy*
2University of Cagliari, Department of Civil and Environmental Engineering and Architecture, Piazza d'Armi, 90123, Cagliari, Italy

(Received February 17, 2014, Revised March 12, 2014, Accepted March 20, 2014)

1. Introduction

The most peculiar characteristic of a conventional radar is its ability to determine the range (i.e. the distance) of a target by measuring the time for the radar signal to propagate to the target and back. Although the name *RADAR* is derived from *RA*dio *D*etection *A*nd *R*anging, it is well-known (Skolnik 1990) that a radar is capable of providing more information about the target than its name would imply and typical applications include the evaluation of the radial velocity, the angular direction, size and shape of the target as well as its dielectric characteristics.

Recent advances in radar technology include the development of microwave interferometers, capable of simultaneously measuring the (static or dynamic) deflection of several points on a large structure with high accuracy (Pieraccini *et al.* 2004). The main ideas of the microwave-based

∗Corresponding author, Associate Professor, E-mail: carmelo.gentile@polimi.it
[a] Ph.D. Student, E-mail: alessandro.cabboi@unica.it

measurement of deflections are:

- to employ a radar, emitting high resolution electromagnetic waveforms (Wehner 1995, Taylor 2001), to take consecutive images of the investigated structure. Each radar image represents a distance map of the intensity of radar echoes coming from the reflecting targets. For example, each discontinuity of a structure (such as the "corner zones" corresponding to the intersection of girders and cross-beams in the deck of bridges) represents a good reflecting target, so that reflecting zones act as a series of virtual sensors;
- to measure the displacement response of each target detected in the scenario by analysing the phase of the back-scattered microwaves collected at different times (Henderson and Lewis 1998).

The practical implementation of the above principles in a sensor prototype was carried out by the Italian company IDS (Ingegneria Dei Sistemi, Pisa, Italy).

After some preliminary tests on full-scale structures (Pieraccini *et al.* 2004), a joint research started between IDS and Politecnico di Milano, mainly aimed at validating the results of the equipment and assessing its performance in ambient vibration tests of bridges (Gentile and Bernardini 2008, Gentile and Bernardini 2010, Gentile 2011). Once the metrological studies of the sensor and the related validation tests on full-scale structures have been performed, the microwave remote sensing could be proposed for the application to structural elements that are difficult to access by using conventional techniques, such as the stay cables in cable-stayed structures (Gentile 2010, Caetano and Cunha 2011).

Structural Health Monitoring (SHM) of cable-stayed bridges currently involves periodic dynamic measurements on stay cables, generally based on the use of accelerometers, since these sensors are very accurate, relatively inexpensive and have adequate technical characteristics. On the other hand, the accelerometers need to be conveniently mounted on the external cable surface and the installation is generally uneasy, time-consuming and might subject the test crew to hazardous conditions if the bridge is in service. Hence, the measurement of cable vibrations has become a standard benchmark for the application of innovative non-contact systems. For example, the laser Doppler technology – firstly used for the measurement of cable vibrations on the Vasco da Gama bridge by Cunha and Caetano (1999) – has been successfully adopted for the assessment of several bridges in the United States, where it has become an accepted tool for fast testing of stay cables (Mehrabi 2006). Other investigations suggest the application of image analysis using digital cameras and field tests have been carried out on cable-stayed bridges and footbridges to demonstrate the reliability of this technique (Ji and Chang 2008, Caetano *et al.* 2011).

Within this context, remote sensing by microwave interferometers seems very promising and exhibits various advantages, when compared to other non-contact techniques, such as (Gentile 2010): (a) possibility of simultaneously measuring the dynamic response of all cables belonging to an array; (b) high accuracy; (c) possibility of usage in almost all weather conditions.

In the first part of the paper, the main techniques adopted in microwave remote sensing are described, in order to highlight advantages and potential issues of the new technology. Subsequently, the paper presents the application of microwave remote sensing to the vibration response measurement on the stay cables of two cable-stayed bridges. In the first case study, one array consisting of two couples of very close stays was tested so that the sensitivity to spacing of targets was investigated. In the second experimental survey, extensive measurements were performed in operational conditions on all stay cables of the curved cable-stayed bridge erected in the commercial harbour of Porto Marghera, Venice, Italy (Gentile and Siviero 2007) by using conventional accelerometers and microwave remote sensing. Two series of tests were conducted

(in July 2010 and April 2011, respectively) with the two-fold objective of demonstrating the accuracy and the operational simplicity provided by the microwave remote sensing and verifying the repeatability of radar survey, with SHM purposes. Furthermore, the comparison between simultaneously collected radar and accelerometer data (which are usually regarded as reference data in dynamic tests) allowed to investigate the errors/uncertainties in radar results.

2. The radar technology and the microwave interferometer

Two main steps are required to simultaneously measure the displacement of several points on a large structure by using a radar (Gentile 2011):

- acquiring consecutive radar images, where different points of the structure are individually observable, at an appropriate sampling rate;
- using the phase variation of the back-scattered microwaves coming from each target point at different times to evaluate the displacement.

The latter task is in principle very simple through the microwave interferometry (see e.g. Henderson and Lewis 1998). For example, let us consider the single degree of freedom system shown in Fig. 1 and a radar emitting a sinusoidal wave. If the target does not move, the phase angle of the radar echo does not change in time; on the other hand, if the mass is vibrating, the received echoes obtained at different times exhibit phase differences, which are proportional to the displacement along the direction of wave propagation. Hence, the displacement d_{LOS} along the radar line of sight is simply computed from the phase shift $\Delta\varphi$ as

$$d_{LOS} = -\frac{\lambda}{4\pi}\Delta\varphi \tag{1}$$

where λ is the wavelength of the electromagnetic signal.

As previously pointed out, the application of microwave interferometry (1) to real structures implies to acquire "images" of the structure at an appropriate sampling rate, with several points on the structure being individually observable in each image. Two or more target points, illuminated by the radar, are individually detectable if they produce different echoes. The *range resolution* or

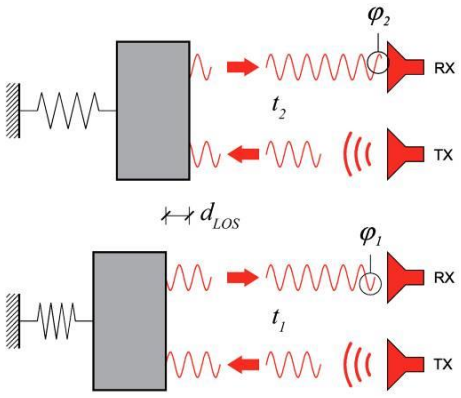

Fig. 1 Schematic representation of radar interferometry

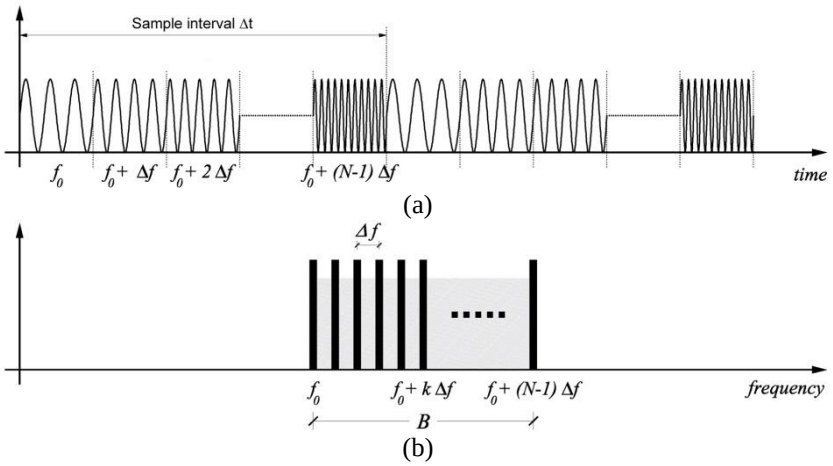

Fig. 2 Representation of a Stepped Frequency Continuous Waveform in (a) time and (b) frequency domain

distance resolution Δr refers to the minimum separation that can be observed along the radar line of sight. The range resolution area is called *range bin*.

Among the radar waveforms (Wehner 1995, Taylor 2001) providing high range resolution, the more usual is probably the short pulse. The shorter the pulse, the more precise is the measurement of the range because the range resolution Δr is related to the pulse duration τ by the following

$$\Delta r = \frac{c\tau}{2} \tag{2}$$

where c is the speed of light in free space. For a pulse of duration τ, the time-bandwidth product satisfies the equality $\tau B = 1$ (see e.g., Marple 1987), where B is the bandwidth (i.e., the width of the range of emitted frequencies). Hence, the range resolution Δr may be expressed as

$$\Delta r = \frac{c}{2B} \tag{3}$$

Eqs. (2) and (3) show that a better range resolution (corresponding to a smaller numerical value of Δr) can be obtained either decreasing τ or increasing B. Instead of using short-time pulses, the Stepped Frequency Continuous Wave (SF-CW) technique (Wehner 1995, Taylor 2001) can be adopted to increase B. SF-CW radars exhibit a large bandwidth by linearly increasing the frequency of successive pulses in discrete steps, as shown in Fig. 2. A SF-CW radar has a narrow instantaneous bandwidth (corresponding to individual pulse) and attains a large effective bandwidth $B = (N-1)\Delta f$ through a burst of N electromagnetic pulses (tones), whose frequencies are increased from tone to tone by a constant frequency increment Δf. It should be noticed that a SF-CW radar emits one burst of N tones at each sample time interval (Fig. 2(b)).

By taking the Inverse Discrete Fourier Transform (IDFT) of the received complex signal sampled at N discrete frequencies, the response is reconstructed in the time domain of the radar: each complex sample in this domain represents the echo from a range (distance) interval of length $c/2B$. The synthetic profile, or range profile, of the radar echoes is then obtained by calculating the magnitude of the IDFT of acquired vector samples. The range profile is simply a 1-D map of the

intensity of radar echoes in function of the distance of the objects that generated the echoes themselves; in other words, it represents a 1-D map of the scattering objects versus their distances.

The concept of range profile is better illustrated in Fig. 3, where an ideal range profile is shown, as obtained when the radar beam illuminates a series of targets at different distances and different angles from the axis of the system. The peaks in the amplitude of the IDFT at each time interval (Fig. 3) identify the position of the targets detected in the scenario, whereas the phase difference between two consecutive IDFTs provides the targets deflection through Eq. (1).

Fig. 3 shows the angle of transmission covered by the main lobe of the antenna in the horizontal plane, with all the points inside the shadowed area of Fig. 3 being observable from the sensor. It is to be noticed that a radar sensor transmits electromagnetic waves also in the vertical plane (see also Figs. 4(b) and 11(a)) and that different transmission angles in the vertical and horizontal plane could be obtained by using different antennas.

Fig. 3 also shows that the radar has only 1-D imaging capabilities, i.e. different targets can be individually detected if they are placed at different distances from the radar. Consequently, measurement errors may arise from the multiplicity of contributions to the same range bin, coming from different points placed at the same distance from the radar but not lying on the same axis (Gentile and Bernardini 2008, Gentile and Bernardini 2010, Rödelsperger *et al.* 2010).

It is worth underlining that the microwave interferometry, represented by Eq. (1), provides a measurement of the displacement of each range bin along the radar line of sight; hence, the evaluation of the actual displacement requires the knowledge of the direction of motion.

In order to provide a simple example of a real range profile, let us refer to the cable-stayed bridge shown in Fig. 4(a), that crosses the river Oglio between the towns of Bordolano and Quinzano, about 70 km far from Milan (Gentile 2010). The deflection response of the two arrays of forestays to wind and traffic excitation was acquired by positioning the microwave interferometer at the base of upstream-side and downstream-side tower, respectively, as shown in Fig. 4(b). Since the position of the sensor is inclined upward, the only targets encountered along the path of the electromagnetic waves are the stays themselves (Fig. 4(b)).

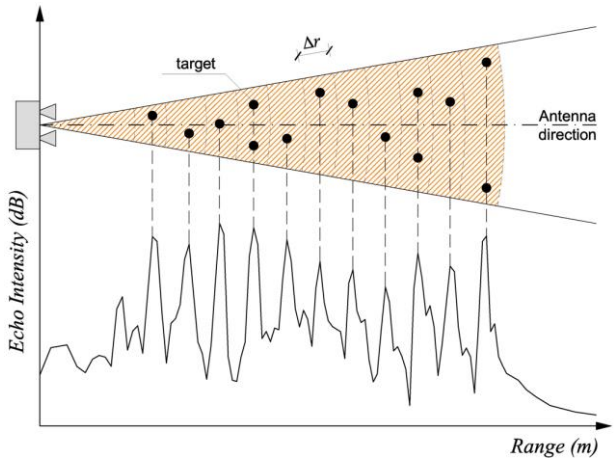

Fig. 3 Idealization of a radar image profile (range profile)

(a)

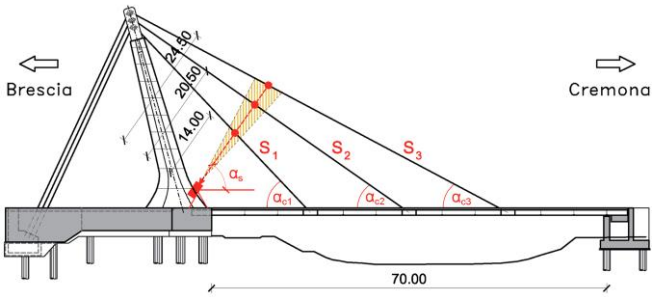

(b)

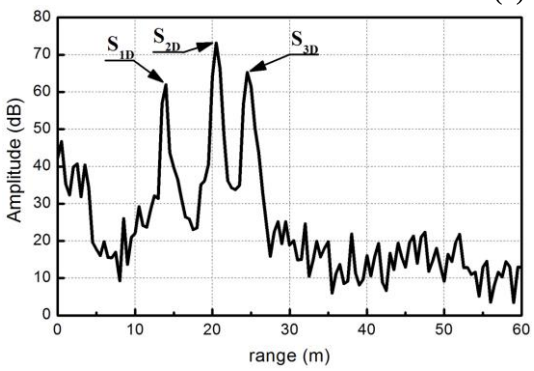

(c)

Fig. 4 (a) View of the cable-stayed bridge between Bordolano and Quinzano (Gentile 2010); (b) Elevation view of the bridge and radar position in the test of forestays (dimensions in m); (c) Range profile of the test scenario on downstream side

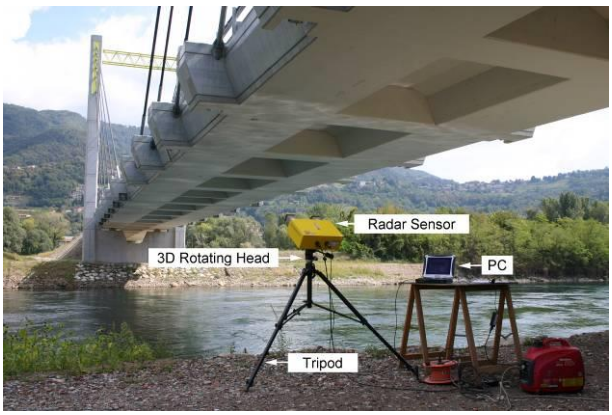

Fig. 5 View of the radar sensor (IDS, model IBIS-S)

Therefore, the range profile exhibits well defined peaks, which correspond to the reflecting targets and clearly identify the position of the cables, as it is shown in Fig. 4(c) for the forestays on the down-stream side. The inspection of Figs. 4(b) and 4(c) reveals that the peaks in the range

profile (indicated as S_{1D}, S_{2D} and S_{3D} in Fig. 4(c)) occur exactly at the expected distances from the sensor (Fig. 4(b)). It should be noticed that the radar sensor can simultaneously detect the displacement response of the reflecting points detected in the scenario and corresponding to the peaks of the range profile.

The radar technology, based on the combined use of SF-CW and microwave interferometry, was implemented in the industrially engineered microwave interferometer (IDS, IBIS-S system) used in this work. The radar equipment (Fig. 5) consists of a sensor module, a control PC and a power supply unit. The sensor module is a coherent radar (i.e., a radar preserving the phase information of the received signal) generating, transmitting and receiving the electromagnetic signals to be processed in order to provide the deflection measurements. The equipment radiates at a central frequency of 17.20 GHz, so that the radar is classified as K_u-band, according to the standard radar-frequency letter-band nomenclature from IEEE Standard 521-1984.

The main technical characteristics of the IBIS-S sensor are the following:

- maximum range (distance) resolution: 0.50 m;
- maximum sampling frequency: 200 Hz;
- maximum operational distance: 500 m;
- displacement accuracy: < 0.02 mm.

It is further noticed that the radar technology provides other advantages including independence of daylight and weather, portability and quick set-up time (about 10 minutes).

On the other hand, obvious issues and sources of uncertainties are related to the 1-D imaging capabilities, not always easy localization of measurement points (geo-referencing of target points), and relative displacements in line of sight only.

3. Microwave remote sensing of stay cables

The periodic dynamic measurements performed on stay cables are aimed at: (1) identifying the local natural frequencies and damping ratios and (2) evaluating the tension forces from natural frequencies and monitoring the changes in these forces over time.

If a linear correlation exists between the mode order n and the corresponding natural frequency f_n of a cable, the tension force T in the cable can be obtained from the natural frequencies using the taut string model (see e.g., Irvine 1981, Caetano 2007)

$$T = 4\rho L^2 \left(\frac{f_n}{n} \right)^2 \tag{4}$$

where ρ is the mass per unit length and L is the effective length of the cable. For stay cables that deviate from a taut string, the cable forces are often (Geier *et al.* 2006) estimated by using the approximate relationship (Morse and Ingard 1986)

$$f_n = \frac{n}{2L} \sqrt{\frac{T}{\rho}} \left[1 + \frac{2}{\xi} + \left(4 + \frac{n^2 \pi^2}{2} \right) \frac{1}{\xi^2} \right] \tag{5}$$

where E and J are the Young's modulus and the inertia moment of the stay cable, respectively, and

$$\xi = L\sqrt{\frac{T}{EJ}} \tag{6}$$

is the dimensionless bending stiffness. Eq. (5) accounts for the effects of the cable bending stiffness: if EJ is assumed to be zero, the dimensionless bending stiffness ξ tends to infinite and Eq. (5) reduces to Eq. (4).

It should be noticed that Eq. (5) is especially suitable for practical applications because T and ξ can be easily estimated from its fit to the series of identified frequencies f_n.

Application of microwave remote sensing to perform systematic dynamic assessment of stay cables seems especially promising for several reasons, such as: (a) the simple, quick and safe way of testing; (b) the possibility of simultaneously measuring the response of several cables; (c) the high accuracy expected from radar-based measurements in terms of both natural frequencies and cable tensions (Gentile 2010); (d) the applicability also in case of fog or rain and in almost all weather conditions and (e) the measurement of the deflection time-history, that could be used directly to evaluate the susceptibility of cables to large amplitude oscillations or the efficiency of devices (e.g. external dampers) adopted to prevent excessive vibrations.

In addition, the possible issues and uncertainties that may occur in the application of the radar technique to bridges and large structures (i.e. 1-D imaging capabilities and *a priori* knowledge of the direction of motion), can hardly affect the survey of an array of cables. More specifically:

1. as already shown in Fig. 4(b), the typical position of the sensor in the survey of an array of cables is inclined upward; hence, the stay cables are the only targets encountered along the path of the electromagnetic waves, so that 1-D imaging capability is perfectly adequate to the test scenario;
2. it can be assumed that the in-plane motion of the *i*-th cable is orthogonal to its axis, so that the actual deflection d_i can be expressed as

$$d_\mathrm{i} = \frac{d_{LOS,\mathrm{i}}}{\cos[\pi/2 - (\alpha_\mathrm{ci} + \alpha_s)]} \tag{7}$$

where α_ci and α_s are the slope of the *i*-th cable and of the sensor, respectively (Fig. 4(b)). In other words, the prior knowledge of the direction of motion is available for cable systems, so that it is possible to evaluate the actual displacement from the one along the line of sight.

However, the SF-CW technique might fail to detect individual cables when applied to arrays with closely spaced stay-cables. In order to investigate this aspect, a quick test was carried out on the forestays of the cable-stayed bridge, shown in Figs. 6(a) and 6(b). The bridge, about 400.0 m long, crosses the Adda river in the neighbourhood of the town of Montodine; the central span of the bridge is supported by 4 arrays of forestays, with each array consisting of 2 couples of closely spaced cables. Fig. 6(b) shows the radar position in the test of one array of forestays: the interferometer was placed at the base of the tower on the Crema side and inclined 65° upward.

The inspection of the range profile, illustrated in Fig. 7, clearly demonstrates that cables S_{01} and S_{02}, only 1.0 m apart, are not individually detected, whereas cables S_{03} and S_{04}, 1.35 m apart, are clearly distinguishable through a couple of closely spaced peaks; therefore, only the deflection time-histories of stay cables S_{03} and S_{04} are correctly provided by the microwave interferometer. Hence, the experimental evidence shows that, although the minimum range resolution of the radar interferometer is in principle equal to 0.5 m, the minimum distance required in the practice to individually detect two targets in a range needs to be larger than twice the minimum range

resolution (i.e., 1.20-1.5 m). It is worth mentioning that this aspect turns out to be independent on the tools commonly adopted in signal processing (such as the windowing used to reduce the side-lobes effects that, in turn, might affect the range resolution).

Fig. 8 shows the auto-spectral density (ASD) associated to the ambient response of cable S_{04} in the vertical plane. The frequency content of the response is characterized by a large number of equally spaced and well-defined peaks in the frequency range 0-30 Hz, so that the tension force can be computed using the taut string model. Application of Eq. (4) (assuming L = 116.82 m and ρ = 85.9575 kg/m) leads to an estimated value of 7044 kN, with the design value being 7000 kN.

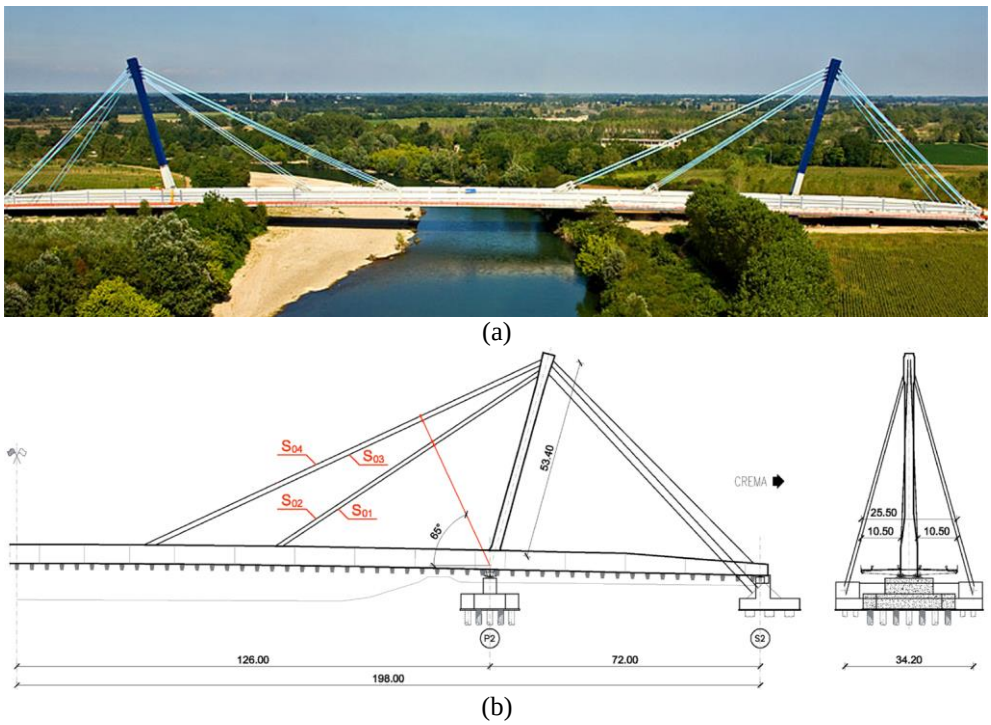

Fig. 6 (a) View of the cable-stayed bridge crossing the Adda river at Montodine; (b) Elevation of the bridge and radar position in the test of forestays (dimensions in m)

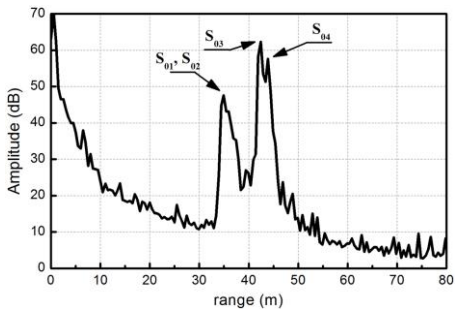

Fig. 7 Range profile of the test scenario corresponding to the forestays of Montodine bridge

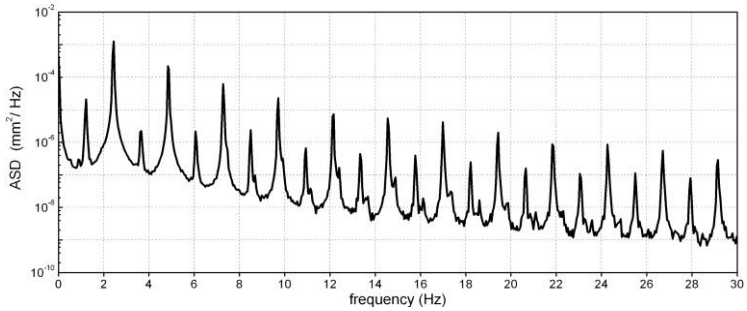

Fig. 8 Auto-spectrum (ASD) of the displacement data measured on cable S04 of Montodine bridge

4. Application to the cable-stayed bridge in Porto Marghera

As previously pointed out, dynamic measurements on stay cables are often aimed at identifying the local natural frequencies. In order to evaluate the reliability and the accuracy of microwave remote sensing, the radar technique was firstly applied to few stays of the "Cesare Cantù" cable-stayed bridge (Fig. 5, Gentile 2010) and to the forestays of the bridge between Bordolano and Quinzano (Fig. 4, Gentile 2010).

More recently, two series of extensive measurements were performed in operational conditions on all stay cables of the curved cable-stayed bridge erected in the commercial harbour of Porto Marghera, Venice, Italy (Figs. 9 and 10, Gentile and Siviero 2007) by simultaneously using accelerometers and interferometric radar.

4.1 General description of the cable-stayed bridge

The cable-stayed bridge (Figs. 9 and 10) belongs to a viaduct, including six spans (42 m + 105 m + 126 m + 30 m + 42 m + 42 m), that generally curves with a radius of 175 m (Fig. 10). The cable-stayed bridge consists of an inclined concrete tower, single-plane cables and a composite deck. The curved deck has a centreline length of 231 m, with two different side spans and 9 cables supporting each side span.

The cast-in-place inclined tower (Fig. 9) is a visually memorable landmark and played a determining role in the conceptual and executive design of the bridge. The tower is about 75 m high and is characterized by a complex geometric layout, where both the base and the height of the triangular cross section are varying along the inclined longitudinal axis.

4.2 Ambient vibration testing of the stay cables and results

Two ambient vibration tests were carried out, in July 2010 and April 2011, on all cables of the bridge with the objective of investigating the accuracy and repeatability of radar survey. The dynamic tests were performed on one array of stay cables at a time and simultaneously using accelerometers and radar interferometer. Fig. 11(a) shows the accelerometers and radar position in the test of the cables on Mestre side. The radar was placed at the cross-section of the deck that is vertically supported by the basement of the tower and inclined 55° upward (Fig. 11)); a similar

set-up was adopted in testing the array of stay cables on the opposite (Venice) side of the bridge.

Fig. 11(a) also shows the angle of transmission covered by the main lobe of the antenna in the vertical plane: as stated in section 2, all the points inside the shadowed area of Fig. 11(a) are observable from the sensor.

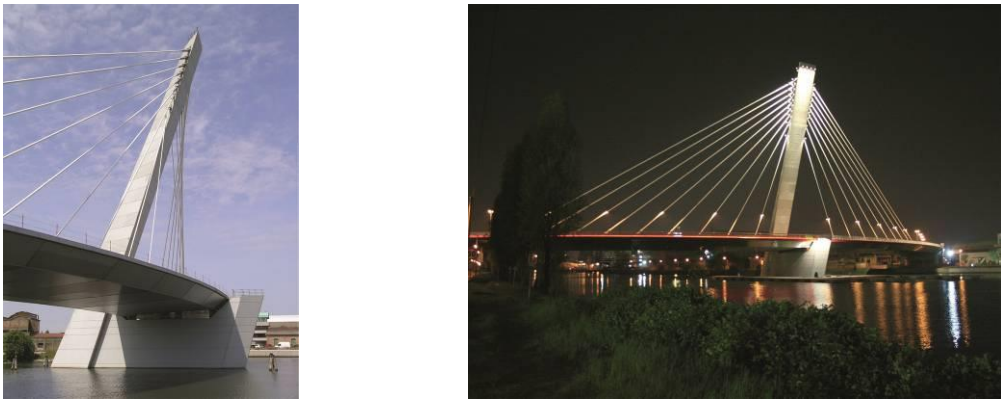

Fig. 9 Views of the cable-stayed bridge in Porto Marghera (Venice, Italy)

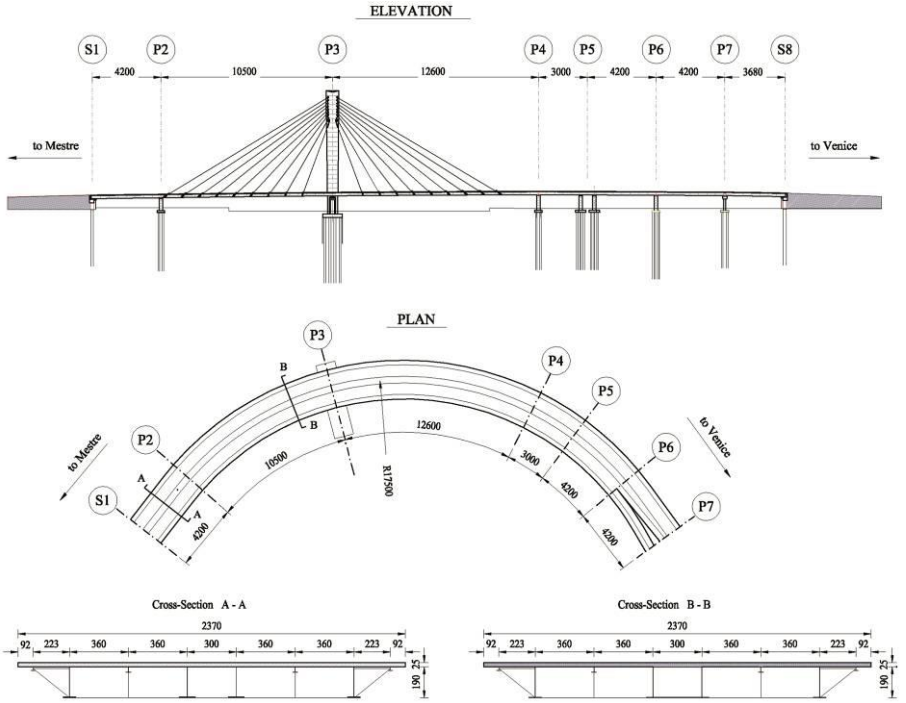

Fig. 10 Elevation, plan and typical cross-sections of the cable-stayed bridge in Porto Marghera

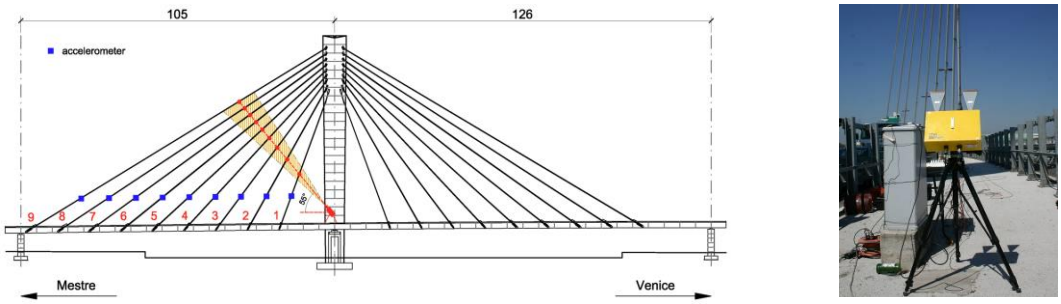

(a) (b)

Fig. 11 Dynamic survey of the array of stay cables on Mestre side: (a) accelerometers and radar position; (b) view of the radar interferometer on site

The range profiles of the test scenarios observed in the two experimental surveys are presented in Fig. 12. Notwithstanding the slightly spatial arrangement of the cables of each array, all the cables are clearly detected in Fig. 12, due to the cone-shaped emission of the sensor in both vertical and horizontal planes. Moreover, the radar image profiles obtained in the two tests for each side are very similar and each range profile exhibits nine well defined peaks, occurring at the expected distance from the sensor and clearly identifying the position in range of the cables.

For each array and for each test, 3000 s of radar and accelerometer data were acquired at a rate of 200 Hz. It is worth mentioning that the maximum deflection of cables (estimated by using the projection expressed by Eq. (7)) was generally lower than 5.0 mm and tends to increase with increased length of the stay cables. Fig. 13 exemplifies 100 s of displacement time-history, recorded on the longer stay of the Mestre side array in the second test (April 2011).

The cable frequencies were identified by computing the auto-spectrum of both acceleration and displacement data. Each collected time-series was low-pass filtered and decimated 5 times; subsequently, the ASD of each re-sampled signal was estimated using the modified periodogram method (Welch 1967). According to this approach, an average is made over each recorded signal, divided into M frames of $2n$ samples, where windowing and overlapping is applied. In the present application, smoothing is performed by 4096-points Hanning-windowed periodograms that are transformed and averaged with 66.7% overlapping. Since the re-sampled time interval is 0.025 s, the resulting frequency resolution is $1/(4096\times0.025) \approx 0.00977$ Hz.

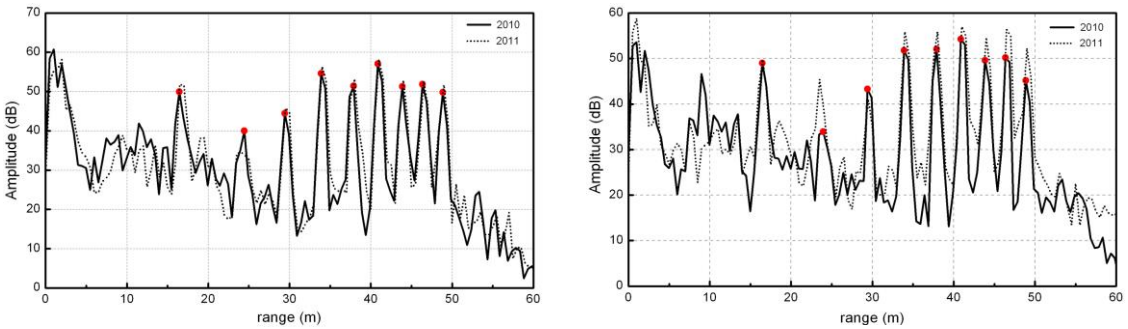

(a) Mestre side (b) Venice side

Fig. 12 Range profile of the test scenarios detected in 2010 and 2011

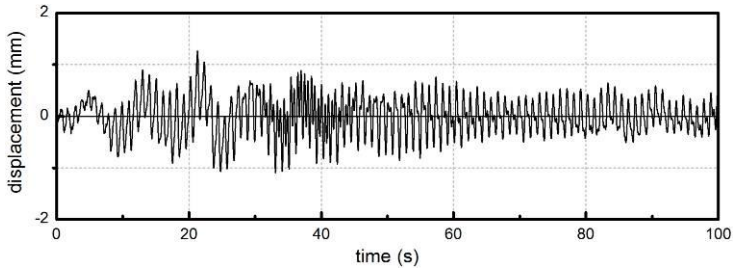

Fig. 13 Sample of deflection time-history measured on the longer stay cable of Mestre side

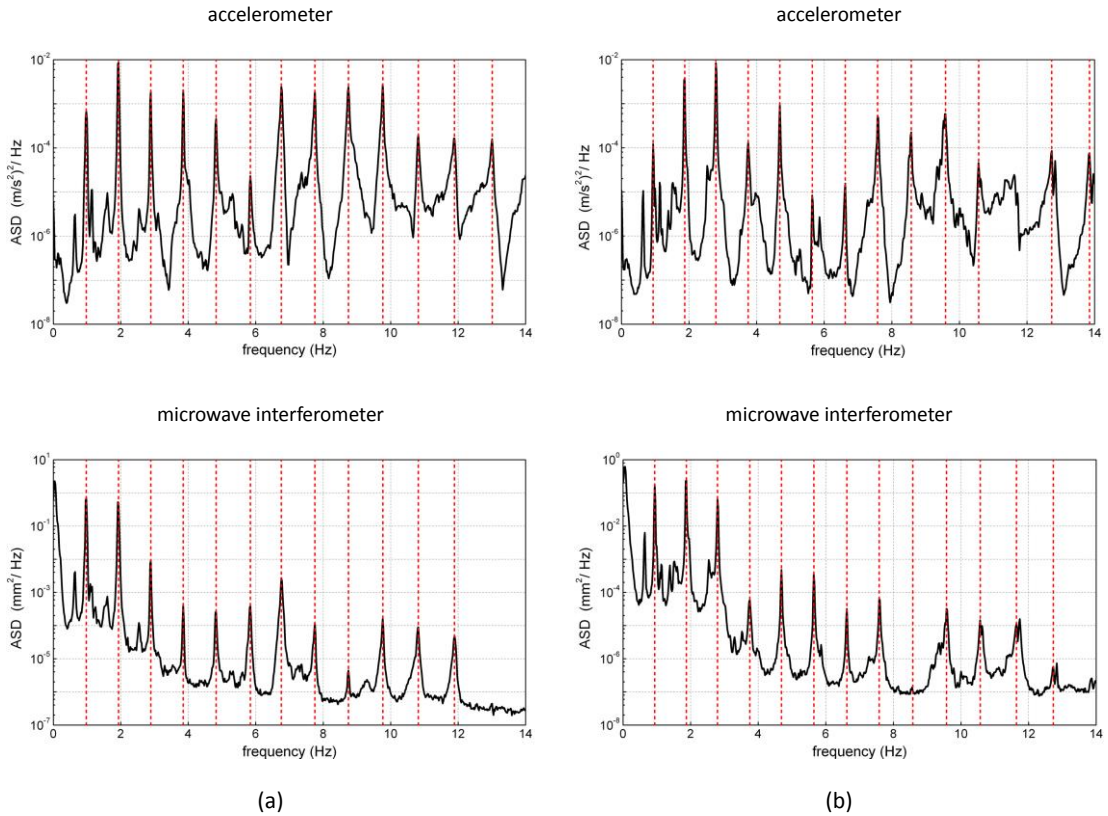

Fig. 14 Auto-spectra (ASD) of acceleration and displacement data measured in 2010 on the longer stays of: (a) Mestre side; (b) Venice side

Fig. 14 shows the ASDs of the ambient responses acquired, by using the two measurement systems, on the longer cables of both arrays during the first test (July 2010). Although the ASDs of Fig. 14 are associated to different mechanical quantities measured (displacement and acceleration) and to different points of the cables, the spectral plots clearly show that a large number of local resonant frequencies are identified from radar data, with these frequencies being practically equal

to the ones obtained from accelerometers.

In order to quantitatively exemplify the correspondence between the results of the two measurement techniques in terms of cable frequencies, Table 1 summarizes the lower 8 natural frequencies, identified from accelerometer and radar data, of the Mestre-side array in the second test (April 2011). Table 1 confirms that microwave remote sensing generally provides a large number of cable frequencies as accurate as those obtained with conventional accelerometers.

Usually, the number of frequencies identified from radar data is large enough to establish if the cable behaves as a taut string or deviate from a taut string; hence, accurate estimate of the cable tensions are likely to be retrieved from the identified natural frequencies as well.

Table 1 Cable frequencies identified from accelerometer and radar data (Mestre side array, April 2011)

Stay Cable n.	Sensor Type	f_n (Hz)							
		$n = 1$	$n = 2$	$n = 3$	$n = 4$	$n = 5$	$n = 6$	$n = 7$	$n = 8$
1	accelerometer	1.230	2.451	3.721	5.068	–	8.203	9.883	11.670
	radar	1.230	2.451	3.721	5.078	–	–	–	–
2	accelerometer	1.211	2.393	3.662	5.029	6.514	8.037	9.707	11.563
	radar	1.211	2.393	3.662	5.029	6.514	–	–	–
3	accelerometer	1.631	3.252	4.873	6.650	8.359	10.137	11.982	13.965
	radar	1.631	3.252	4.873	6.660	8.369	10.166	–	13.965
4	accelerometer	1.533	3.076	4.648	6.240	7.861	9.521	11.230	12.988
	radar	1.533	3.076	4.648	6.240	7.861	9.512	11.230	12.998
5	accelerometer	1.387	2.764	4.160	5.537	7.090	8.574	10.088	11.660
	radar	1.387	2.764	4.150	5.537	7.090	8.574	10.098	11.660
6	accelerometer	1.289	2.578	3.887	5.195	6.514	–	9.189	10.566
	radar	1.289	2.578	3.887	5.195	6.504	–	9.189	10.566
7	accelerometer	1.240	2.480	3.721	4.961	6.260	7.520	8.789	10.146
	radar	1.240	2.480	3.721	4.961	6.260	7.520	8.789	10.146
8	accelerometer	1.104	2.197	3.301	4.414	5.527	6.650	7.764	8.906
	radar	1.104	2.197	3.301	–	5.537	6.650	7.764	8.916
9	accelerometer	0.967	1.924	2.881	3.848	4.814	5.830	6.768	7.754
	radar	0.967	1.924	2.881	3.848	4.814	5.830	6.768	7.754

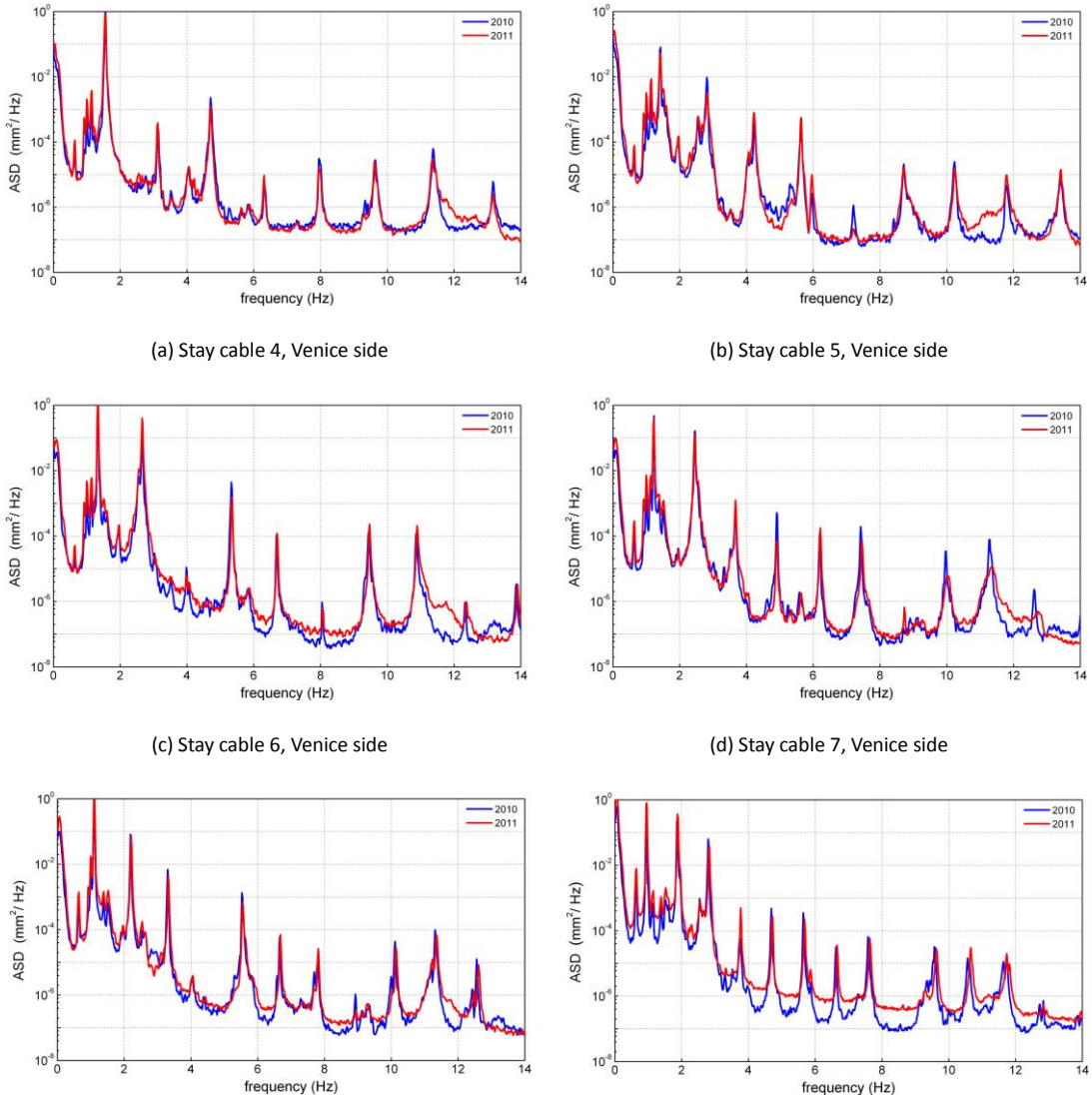

(a) Stay cable 4, Venice side

(b) Stay cable 5, Venice side

(c) Stay cable 6, Venice side

(d) Stay cable 7, Venice side

(e) Stay cable 8, Venice side

(f) Stay cable 9, Venice side

Fig. 15 Auto-spectra (ASD) of the displacement data measured in 2010 and 2011 on stays 4-9, Venice side

It is worth underlining that similar results, in terms of number and agreement of natural frequencies, have been obtained for all the stay cables of the two arrays in both tests, with the exception of the two shorter ones (cables 1-2 in Fig. 11(a)). For the shorter stays, the radar technique detected the lower 3-5 local natural frequencies only, whereas the accelerometers provided a larger number of cable frequencies (Table 1). This specific aspect, firstly observed in the test of July 2010, was subsequently investigated in April 2011 and the main reason of the different performance of the two measurement techniques on the shorter stays was found to be

related to the different electromagnetic reflectivity of the protective sheath. Another factor that might reduce the reflectivity of the shorter stays is related to their slope with respect to radar line of sight (since the radar cross section of a long cylinder is maximum when the line of sight is orthogonal to the cylinder axis).

Fig. 15 refers to stay cables 4-9 on Venice side and compares the ASDs associated to the deflection response measured in 2010 and 2011. The spectral plots in Fig. 15 are a synthesis of the frequency content present on those cables in the two tests, and indicate that the local natural frequencies of the longer cables 7-9 tend to slightly increase in the second test.

The summary of identified frequencies (Table 1) also allows to conclude that the bridge cables slightly deviate from the taut string, so that Eq. (5) was preferred to estimate the cable forces. The tension force T and the dimensionless bending stiffness ξ of each stay cable were determined by minimizing the difference between the natural frequencies predicted by Eq. (5) and the experimental ones. For each cable, all the experimentally identified natural frequencies were used in the least square minimization procedure.

The application of Eq. (5) to the natural frequencies identified from accelerometer and radar data collected in 2010 and 2011 leads to the cable tensions summarized in Table 2: as expected from the agreement of cable frequencies, practically the same cable forces were estimated using radar and accelerometer data, except for some shorter stay-cables where only a few natural frequencies were estimated from radar data.

Table 2 also highlights that, between the two tests, the cable forces turned out to be practically unchanged on Mestre side, whereas slight changes were detected on Venice side, where the tension force tends to decrease in lower cables (3-5) and to increase in longest cables (7-9).

Table 2 Cable forces identified from accelerometer and radar data in the tests of June 2010 and April 2011

	Sensor Type	Mestre side, Stay cable n.								
		1	2	3	4	5	6	7	8	9
T^{2010} (kN)	accelerometer	455	755	2350	3721	3866	4190	4825	5294	4746
	radar	446	699	2394	3720	3871	4188	4781	5306	4745
T^{2011} (kN)	accelerometer	458	757	2359	3715	3842	4199	4828	5289	4771
	radar	436	703	2386	3712	3863	4196	4795	5295	4770
	Sensor Type	Venice side, Stay cable n.								
		1	2	3	4	5	6	7	8	9
T^{2010} (kN)	accelerometer	647	906	2414	3771	4005	4324	4588	5275	4512
	radar	690	837	2435	3774	4005	4324	4580	5280	4522
T^{2011} (kN)	accelerometer	614	860	2381	3704	3961	4352	4698	5310	4655
	radar	690	837	2378	3736	3976	4346	4698	5312	4635

5. Conclusions

The paper focuses on the application of microwave remote sensing to the measurement of dynamic deflections on the cables of cable-stayed bridges. The dynamic tests were performed in operational conditions and the maximum deflections of the stay cables were generally lower than 5.0 mm (i.e., more than 200 times larger than the displacement accuracy of the radar sensor).

Based on the presented results and the extensive comparison between simultaneously collected radar and accelerometer data, the following conclusions can be drawn:

1. the typical errors and uncertainties that might pollute the quality of radar measurement of deflections (i.e., 1-D imaging capabilities, uncertainties in the identification of reflecting targets and relative displacement in line of sight only) do not affect the dynamic survey of stay cables, especially if the test is aimed at identifying the local natural frequencies of the cables with SHM purposes;
2. the radar technique allows to simultaneously measure the dynamic response of all cables belonging to an array, even when the array is characterized by spatial arrangement and a large number of stay cables;
3. although possible issues may arise from low electromagnetic reflectivity of the cable protective sheath or closely spaced cables, the radar survey exhibits a high degree of repeatability so that it turns out to be especially suitable to the SHM of stay cables;
4. a large number of natural frequencies can be identified from radar data on each cable of an array and the cable frequencies seem as accurate as those obtained with conventional accelerometers;
5. in the investigated case studies, the number of cable frequencies identified from radar data was generally sufficient to establish if the stay cables behave as a taut string or deviate from a taut string, so that accurate estimate of the cable tensions can be retrieved from the identified natural frequencies.

Since the advantages of remote sensing using microwave interferometers also include independence on daylight and weather conditions, high spatial resolution, portability and quick set-up time, the radar interferometry probably represents the most powerful and easy-to-use experimental technique, currently available for systematic and accurate evaluation of cable frequencies and tensions.

On the other hand, the evaluation of actual displacement (from the one in line of sight) needs a prior knowledge of the cable's direction of motion as well as reliable geometric information on the slope of the stay cable. Possible measurement errors related to those aspects might be conveniently evaluated by simultaneously using microwave interferometer and geodetic sensors measuring 3D deflections for relatively low frequencies (see e.g. Psimoulis *et al.* 2008, Psimoulis and Stiros 2013) or two radar sensors installed in the same plane at different positions (for example, on the deck and at the base of towers).

Acknowledgments

The support of IDS (Ingegneria Dei Sistemi, Pisa, Italy) in supplying the IBIS-S radar sensor employed in the tests is gratefully acknowledged.

M. Antico and M. Cucchi (VIBLAB, Politecnico di Milano) are gratefully acknowledged for the assistance in conducting the field tests.

References

Caetano, E. (2007), *Cable Vibrations in Cable Stayed Bridges*, SED 9, IABSE.

Caetano, E. and Cunha, A. (2011), "On the observation and identification of cable-supported structures", *Proceedings of the 8th International Conference on Structural Dynamics - EURODYN 2011*, Leuven, Belgium, July.

Caetano, E., Silva, S. and Bateira, J. (2011), "A vision system for vibration monitoring of civil engineering structures", *Exp. Tech.*, **35**(4), 74-82.

Cunha, A. and Caetano, E. (1999), "Dynamic measurements on stay cables of cable-stayed bridges using an interferometry laser system", *Exp. Tech.*, **23**(3), 38-43.

Geier, R., De Roeck, G. and Flesch, R. (2006), "Accurate cable force determination using ambient vibration measurements", *Struct. Infrastruct. E.*, **2**(1), 43-52.

Gentile, C. (2010), "Deflection measurement on vibrating stay cables by non-contact microwave interferometer", *NDT & E Int.*, **43**(3), 231-240.

Gentile, C. (2011), "Vibration measurement by radar techniques", *Proceedings of the 8th International Conference on Structural Dynamics - EURODYN 2011*, Leuven, Belgium, July.

Gentile, C. and Bernardini, G. (2008), "Output-only modal identification of a reinforced concrete bridge from radar-based measurements", *NDT & E Int.*, **41**(7), 544-553.

Gentile, C. and Bernardini, G. (2010), "An interferometric radar for non-contact measurement of deflections on civil engineering structures: laboratory and full-scale tests", *Struct. Infrastruct. E.*, **6**(5), 521-534.

Gentile, C. and Siviero, E. (2007), "Dynamic characteristics of the new curved cable-stayed bridge in Porto Marghera (Venice, Italy) from ambient vibration measurements", *Proceedings of the 25th International Modal Analysis Conference (IMAC-XXV)*, Orlando (FL), USA, February.

Henderson, F.M. and Lewis, A.J. (Eds). (1998), *Manual of Remote Sensing. Principles and Applications of Imaging Radar*, Wiley & Sons.

Irvine, M. (1981), *Cable Structures*, MIT Press.

Ji, Y.F. and Chang, C.C. (2008), "Nontarget image-based technique for small cable vibration measurement", *J. Bridge Eng. - ASCE*, **13**(1), 34-42.

Marple, S.L. Jr. (1987), *Digital Spectral Analysis with Applications*, Prentice-Hall.

Morse, P. and Ingard, K. (1987), *Theoretical Acoustics*, Princeton University Press.

Mehrabi, A.B. (2006), "In-service evaluation of cable-stayed bridges, overview of available methods, and findings", *J. Bridge Eng.- ASCE*, **11**(6), 716-724.

Pieraccini, M., Fratini, M., Parrini, F., Macaluso, G. and Atzeni, C. (2004), "Highspeed CW step-frequency coherent radar for dynamic monitoring of civil engineering structures", *Electron. Lett.*, **40**(14), 907-908.

Psimoulis, P., Pytharouli, S., Karambalis, D. and Stiros, S. (2008), Potential of Global Positioning System (GPS) to measure frequencies of oscillations of engineering structures", *J. Sound Vib.*, **318**(3), 606-623.

Psimoulis, P. and Stiros, S. (2013), "Measuring deflections of a short-span railway bridge using a robotic total station", *J. Bridge Eng.- ASCE*, **18**(2), 182-185.

Rödelsperger, S., Läufer, G., Gerstenecker, C. and Becker, M. (2010), "Monitoring of displacements with ground-based microwave interferometry: IBIS-S and IBIS-L", *J. Appl. Geodesy*, **4**, 51-54.

Skolnik, M.I. (Ed.) (1990), *Radar Handbook*, McGraw-Hill.

Taylor, J.D. (Ed.) (2001), *Ultra-wideband Radar Technology*, CRC Press.

Wehner, D.R. (1995), *High-resolution Radar*, Artech House.

Welch, P.D. (1967), "The use of Fast Fourier Transform for the estimation of Power Spectra: a method based on time averaging over short modified periodograms", *IEEE Trans. Audio Electro-Acoust.*, **15**(2), 70-73.